ELSEVIER

Research Paper

Measuring heavy metal ions in water using nature existed microalgae as medium based on terahertz technology

Yongni Shao [a, b], Yutian Wang [a], Di Zhu [a], Xin Xiong [a], Zhengan Tian [d], Alexey V. Balakin [a, c], Alexander P. Shkurinov [a, c], Duo Xu [e], Yimei Wu [f], Yan Peng [a, b, *], Yiming Zhu [a, b, *]

[a] Terahertz Technology Innovation Research Institute, Terahertz Spectrum and Imaging Technology Cooperative Innovation Center, Shanghai Key Lab of Modern Optical System, University of Shanghai for Science and Technology, 516 JunGong Road, Shanghai 200093, China
[b] Shanghai Institute of Intelligent Science and Technology, Tongji University, Shanghai 200092, China
[c] Department of Physics and International Laser Center, Lomonosov Moscow State University, Leninskie Gory 1, Moscow 19991, Russia
[d] Shanghai International Travel Healthcare Center, Shanghai Customs District, 200335, China
[e] Department of Culture, Media & Creative Industries, Faculty of Arts & Humanities, King's College Lonson, WC2R 2LS London, United Kingdom
[f] College of Foreign Languages, University of Shanghai for Science and Technology, Shanghai 200093, China

ARTICLE INFO

ABSTRACT

Heavy metal pollution in water seriously affects human health. The disadvantages of traditional metal ion detection methods involve long and cumbersome chemical pretreatment in the early stage, and large volume of samples. In this study, microalgae were used as the medium, and terahertz spectroscopy technology was employed to collect the changes of material components in it, so as to deduce the types and concentrations of heavy metal pollution in water. Through the partial least square(PLS), we establish the prediction model of heavy metal concentration, and the results show that the best detection time for Pb^{2+} is 6 h and Ni^{2+} is 18 h. The principal component analysis(PCA) shows that β-carotene is the most affected substance. Afterward we collect five real surface waters in East China and verify that the judgment accuracy of Pb^{2+} and Ni^{2+} are 100% and 93.2% respectively. The results indicate that the time is shorter than the traditional pretreatment time from more than 20–6 h, the sample volume is reduced from 50 mL to 10 mL, the detection accuracy is improved from 10 ng/mL to 1 ng/mL. In a word, we provide a new fast and real-time method for biological monitoring of heavy metal pollution in water.

1. Introduction

Due to the urban development and global industrialization, there is an increasing contamination in water, the content of heavy metals in water bodies mainly includes cadmium (Cd), lead (Pb), nickel (Ni), copper (Cu), etc (Mathew and Krishnamurthy, 2015). Which results in serious harm to animals, plants and public health. For instance, long-term exposure to nickel will cause human skin to fester and even the hair will turn white Kobielska et al. (2018). Lead will accumulate in the human body, affect the development of red blood cells and cause leukemia (Mangadze et al., 2019). The persistence and non-degradation of heavy metals as well as the increasing harm from the enrichment of the food chain call for enhancing attention to the problem of heavy metal pollution in water (Ogburn and Vogt, 2017).

At present, atomic absorption spectroscopy (AAS), high performance liquid chromatography (HPLC) etc. are the mainstream approaches for heavy metals detection in water. The disadvantages of these methods include: long and cumbersome chemical pretreatment in the early stage, and large volume of samples. Table 1 shows some parameters of traditional methods for detecting heavy metals. Due to the disadvantages of traditional detection methods and the inability to directly evaluate the impact of heavy metal pollution on biological mechanism, biological monitoring of water environment pollution has become a new research direction. Biological monitoring refers to reflecting the pollution status of water body by detecting the changes of designated organisms polluted by water body (Mangadze et al., 2019). Microalgae is an important photosynthetic organism in the water environment and the largest primary producer group in the world. Its characteristics of fast growth, low cost, easy operation, no pollution and the

Table 1
Parameters of traditional detection methods.

Methods	Pretreatment time	Lower detection limit	Required sample size	Test metal type
Atomic absorption spectroscopy (GB/T 7475–1987; GB/T 11912/1989)	> 20 h	10 ng/mL	> 50 mL	One at a time
High performance liquid chromatography-photometry (Rekhi et al., 2017)	> 20 h	10 ng/mL	> 30 mL	One at a time
Microalgae by THz	6–18 h	1 ng/mL	10 mL	Two at a time

ability to adsorb heavy metals make microalgae an ideal choice for biological monitoring of water pollution (Adhiya et al., 2002; Patel et al., 2019; Stehle et al., 2012).

Generally, heavy metals can be absorbed by microalgae in two forms. One of the forms is developed on the cell surface which we view this process as passive adsorption, through physical and chemical action to adsorb heavy metals, that is to say, metal ions are bound to microalgae through complexation, chelation, ion exchange, physical adsorption, redox, and microprecipitation, which does not depend on cell energy metabolism. The other form occurs within the cell which we call it biosorption, in this case metal ions mainly rely on diffusion for intracellular transport, which is often accompanied by energy consumption (Adhiya et al., 2002; Filote et al., 2019; Subramaniyam et al., 2016). Research by Alicja et al. found that in the zinc solution, the biochemical components of Spirulina adsorbed heavy metals will change. Among them, phycocyanin, chlorophyll a, carotenoids and zinc have the most accumulation, and at different concentrations, the changes of those components are also different (Piotrowska-Niczyporuk et al., 2015). Filote et al. used Spirulina to adsorb Pb^{2+} in waste water (Filote et al., 2019). Adhiya et al. found that heavy metal ions can affect the synthesis of carotenoids in microalgae(Adhiya et al., 2002). Doshi et al. found that the adsorption capacity of algae for Cu^{2+} and Ni^{2+} is much higher than that of activated carbon (Doshi et al., 2006). Ponnuswamy et al. studied the adsorption capacity of Chlorella to Cu^{2+} (Indhumathi et al., 2018). Sultana et al. used Chlorella to adsorb a variety of heavy metals in wastewater, and studied its removal rate of heavy metals (Sultana et al., 2020). The mechanism of biosorption is used in this experiment. After microalgae adsorb heavy metal ions, the composition of substances in the body will change accordingly. Based on the above research findings, using microalgae as a carrier, the correlation between the change trend of substances in the body, including pigments, oils and polysaccharides, and the types and concentrations of heavy metals can be established, so as to invert the pollution situation of heavy metals in water.

Traditional detections on microalgae content usually use spectrophotometer, high performance liquid chromatography, etc., but there are disadvantages such as complicated extraction steps involved. In addition to the traditional detection methods mentioned above, spectroscopy technology is being used in biomedical research due to its fast and non-destructive detection characteristics, mainly including hyperspectral technology, infrared spectroscopy technology, and Raman spectroscopy technology. Hyperspectral imaging technology can not only obtain the spatial position of the object, but also extract the spectral information of the object, among which, the spectral information can provide information of the internal physical structure and chemical composition of the object for analysis, and the image data mainly reflects the external characteristics such as the shape, size and color of the object (Ljungqvist et al., 2013; Wallays et al., 2009; Xing et al., 2010). Infrared spectrum absorption is mainly caused by the transition between different energy levels after the state of molecular vibration, expansion and contraction changes. Among them, the absorption inten-

sity and absorption band of different substances in the near-infrared light are different, so the absorption peak position and intensity are also different in the infrared spectrum(Lohumi et al., 2015; Magwaza et al., 2012). Shao et al. (2015) used visible/near infrared technology to detect spirulina β-carotene. Raman spectroscopy can reflect the differences in the chemical composition and molecular structure of samples at the molecular level. The detection mechanism is different from that of infrared spectroscopy, and it mainly has a strong recognition of nonpolar groups (such as C═C, C-C, etc.). Ji et al. (2014) used Raman spectroscopy to achieve rapid and non-destructive quantitative detection of Chlamydomonas reinhardtii starch). Barlow et al. used hyperspectral coherent anti-Stokes Raman scattering microscopy technology to present the distribution of carotenoid of the Haematococcus pluvialis cells in non-invasive and quantitative way in real time. These studies show that the use of spectroscopy technology to detect and analyze microalgae components is feasible and practical.

With the development of photonics technology and material science and technology, the application research of terahertz radiation technology has rapidly expanded to more and more fields(Shao et al., 2021b). Terahertz (THz) waves are located between far-infrared and microwaves, and the frequency range covers 0.1–10 THz. It has both infrared wave characteristics and microwave characteristics. In addition, compared with other spectroscopic techniques, terahertz waves can penetrate most non-polar materials, and the resonance frequency of the vibration and rotation frequencies of biological macro molecules is in the terahertz band, which is suitable for biopsy of biological tissues (Peng et al., 2020a; Peng et al., 2020b). Many biological samples such as lipids, proteins and other molecules have molecular vibrations in the terahertz range, and their terahertz characteristic peaks are obvious (Nakajima et al., 2019; Yang et al., 2016). In the use of terahertz technology to detect biological components, Dean et al. used Fourier Transform Infrared Spectroscopy (FTIR) to study the content of oil and starch in microalgae over time, and the results showed that FTIR is a reliable method for high-throughput determination of lipid and starch synthesis in microalgae (Dean et al., 2010). Zhang et al. (2010) found that at room temperature β- carotene has a terahertz absorption peak at 17.5 THz. Stehle et al. (2012) found that the terahertz characteristic peak of protein is 3.5–5 THz. Jiang et al. (2011) found that the characteristic peak of lipid was near 9.8 THz (Ling et al., 2012). Nakajima et al. (2019) found that the terahertz characteristic peak of starch was 9.1 THz (Flores-Morales et al., 2012). The above studies showed that the main components of microalgae can be detected by using terahertz spectrum technology, but they just only detected markers. In this study, we used the theory of microalgae biosorption of heavy metals, microalgae were used as the medium, and terahertz technology was adopted to collect the changes of material components in it, so as to deduce the types and concentrations of heavy metal pollution in water. This method has a great application in practical environmental pollution detection.

We divided heavy metals into two categories: highly toxic and generally toxic (Kim et al., 2019). We selected Pb^{2+} to represent highly toxic heavy metal ions and Ni^{2+} to represent less toxic heavy metal ions. We used Scenedesmus obliquus as a biological medium, cultured for 6 h, 12 h and 18 h under different concentrations of lead ions and nickel ions, and collected terahertz band spectra with FTIR, respectively. By analyzing the spectral changes of protein, lipid, starch and carotene in microalgae, combined with PCA, PLS and chemical methods, the time point and corresponding material band in microalgae that are mostly affected by lead ions and nickel ions are obtained. Then, the lead-nickel ion mixed solution was used to stress the microalgae, and the time and band of the above conclusions were used to establish the PLS model. At the same time, we collected five representative actual surface water samples from East China, which were from Taihu Lake, Chaohu Lake, Yangcheng Lake, Hongze Lake and Suzhou Battery Factory' treating waste liquid, and used atomic absorption spectrometry as

standard verification, and obtained good results. This proves that heavy metal ions can be judged directly on surface water. Our flow chart is shown in Fig. 1. We really demonstrate this method and compare with atomic absorption spectroscopy method. We compared it with the traditional methods for detecting heavy metals, as shown in Table 1. We provide a new detection approach and technical support for the real-time monitoring of the types and concentrations of heavy metals in water.

2. Material and methods

2.1. Sources of biological and chemical materials

Scenedesmus obliquus (*Scenedesmus obliquus*, strain 276) used in the experimental study was purchased from the Wildlife Germplasm Bank of the Chinese Academy of Sciences-Freshwater Microalgae Species Bank. The chemical reagents lead nitrate (99%, AR, molecular weight 331.21) and nickel nitrate hexahydrate (98%, AR, molecular weight 290.81) used in the experiment were purchased from Aladdin Reagent Network.

2.2. Microalgae cultivation and sample preparation

Scenedesmus obliquus is a freshwater microalgae culture specimen purchased from the Institute of Aquatic Biology of FACHB-collection, which is expanded in standard BG11 medium autoclaved at 121 °C. The incubation temperature is 25 °C, the light intensity is 3000 Lux, the light versus dark cycle is 12 h:12 h.

Scenedesmus obliquus was cultured for about 2 months until it grew into a stable growth period. In the experiment, 5 equal parts of Scenedesmus obliquus were centrifuged, the supernatant was discarded, and the same amount of ultrapure water was added to repeat the centrifugation three times, the supernatant was discarded, and finally the microalgae mud with impurities removed was harvested.

According to the experimental protocol, we cultivated the microalgae in BG11 (without Pb^{2+} and Ni^{2+}) culture medium, and added the corresponding concentration of heavy metal ion salt crystals to dissolve in the solution under stress. BG11 culture medium was selected as the control medium. The experiment used Scenedesmus obliquus after two months of stable growth, take 10 mL of microalgae suspension for each sample preparation, centrifuge it, add ultrapure water, shake well, and repeat the centrifugation three times for washing. The microalgae mud is ground and broken and placed in a mold. The specification of the mold is 2 cm * 2 cm, the height is 0.5 cm, and the material is polyethylene. After drying at 40 °C for 4 h to prepare film samples.

2.3. Hot ethanol method

Use the hot ethanol method to determine β-carotene, the specific steps are as follows:

(1) Sample preparation: Take 1 mL of the microalgae suspension in a 2 mL centrifuge tube, centrifuge at 6500 r/min for 10 min, and remove the supernatant.
(2) Put the microalgae mud obtained after centrifugation into a refrigerator at − 30 °C and freeze for more than 4 h.
(3) Extraction: add 1 mL of 95% ethanol each time to the sample from which the supernatant is removed, in a water bath for 10 min, and the temperature of the water bath is 80 °C. After mixing the microalgae and ethanol in a water bath, shake it well, and place it in an ultrasonic water bath, avoid light and ultrasonic for 15 min to make the solvent and the microalgae mix uniformly. The sample was taken out and placed at room temperature and protected from light for about 4 h for pigment extraction, then the sample was centrifuged at a speed of 10000r/min for 5 min in a high-speed centrifuge.
(4) Color comparison: Take the sample supernatant after centrifugation, and use 95% ethanol solution as a reference for color comparison. Use an enzyme-labeled instrument to measure the absorbance values at 470 nm and 666 nm respectively.
(5) Calculation of β-carotene content:

$$\beta - carotene = \left(1000A_{470} - 44.76A_{666}\right) vl/V$$

Among them, β-carotene represents the content of β-carotene (mg/L), and A_i represents the absorbance value in the i-band. v represents the volume of organic solvent (mL), V represents the volume of microalgae liquid (mL), and l represents the optical path of the measuring cell (cm). In this experiment, l is 1 (Shao et al., 2021a).
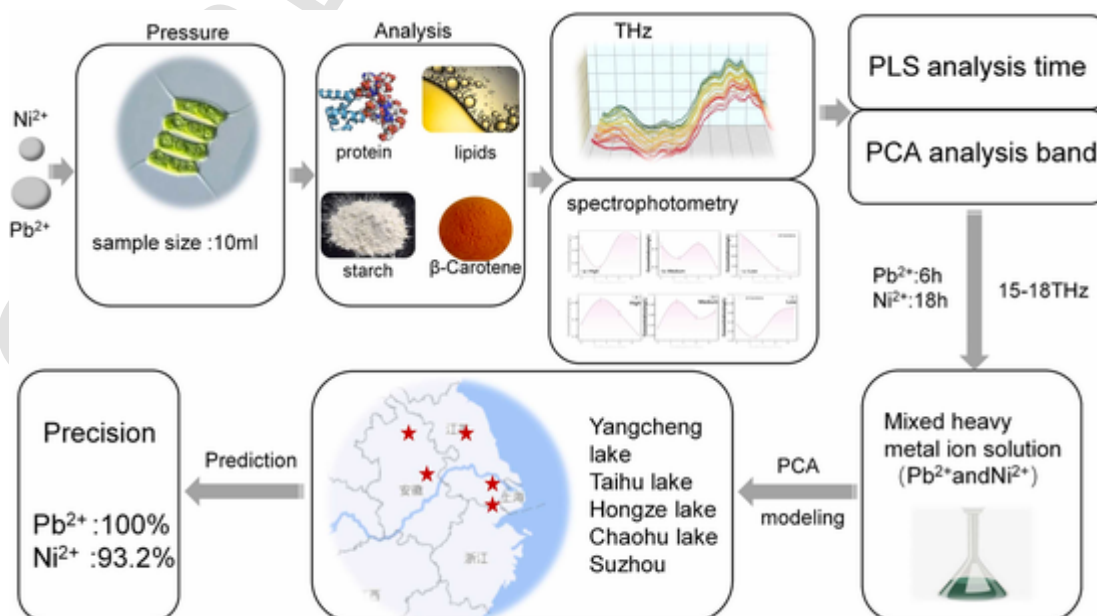
Fig. 1. The approximate flow chart of the study.

2.4. THz spectral measurement

Fourier transforms infrared spectrometer (FTIR) (Vertex 80 v, BRUKER Vertex, Germany) was used to measure the absorption spectrum. The light source is a water-cooled mercury lamp and is detected by a DLaTGS/polyethylene detector. The spectral region covers 0.9–20 THz effectively, and the signal-to-noise ratio (SNR) is better than 10000: 1. The resolution of the spectrometer is 0.12 THz and each spectrum is the average of 128 sample scans performed at a scan speed of 5 kHz on the basis of 128 background scans. To eliminate the effects of moisture, the instrument was filled with nitrogen throughout the data collection process. The jitter rate during measurement is less than 3%, which has good scanning accuracy. Before testing, a blank carrier was placed on the fixture for background scanning and to eliminate the background noise. Scans were recorded using the spectroscopic software OPUS (BRUKER, Germany).

2.5. Principal component analysis (PCA)

Principal component analysis (PCA) is a data processing method which is usually used in multivariate statistical analysis. This method reduces the dimensionality of the data (Leborans and Novillo, 1996), making it more straightforward to identify the main elements among huge amount of data and reduce the complexity of the analysis process. The purpose of this method is to simplify the mathematical model and improve the efficiency of data analysis.

2.6. Partial least squares (PLS)

Partial least squares (PLS) is a multiple linear regression approach utilizing input values and predicted values. It uses the correlation coefficient of the predicted value to find the best solution between the data and the model. Multiple regression analysis is utilized to improve the prediction accuracy level of model(Wang et al., 2010). In the evaluation, the coefficient of determination(R^2) and the root mean square error (RMSE) are usually used to evaluate the performance and reliability of the model.

3. Results and discussions

3.1. Terahertz spectra of Scenedesmus obliquus

Studies have shown that protein, lipid, starch and β-carotene have their own characteristic peak frequency ranges in the terahertz and far infrared bands. The main components of Scenedesmus obliquus are protein, pigment (such as chlorophyll, β-carotene, astaxanthin), starch, lipid, etc. They have different terahertz spectra and are distributed in different frequency bands. In Zhang's research, it revealed that in the 10–20 THz frequency band, and at room temperature, β-carotene had some moderate intensity terahertz peaks, such as 17.5 THz (Zhang et al., 2010). In addition, the characteristic peak of protein was ranging from 3.5 to 5 THz (Stehle et al., 2012). 2.3 THz and the range from 9.2 to 9.8 THz were the characteristic peak for lipid (Jiang et al., 2011; Ling et al., 2012), while the characteristic peak of starch was at 10.5 THz (Flores-Morales et al., 2012; Nakajima et al., 2019). Based on the above results, it indicates that it is feasible to use microalgae as a medium to analyze the spectral changes of microalgae's components, and it can be helpful to study the types and concentration of heavy metals polluted water.

3.2. Spectra of microalgae under Pb²⁺ solution stress

According to the toxicity classification of heavy metals, we selected the weaker toxic ion as Ni^{2+} and the stronger toxic ion as Pb^{2+} according to the toxicity of heavy metals ions. In this study, terahertz spectra acquisition and spectral peak analysis were performed on the samples of Scenedesmus obliquus adsorbed Pb^{2+} in different concentrations of Pb^{2+} solutions. The concentration of Pb^{2+} in the solution was 1 ng/mL, 10 ng/mL, 50 ng/mL, 0.1×10^3 ng/mL, 0.5×10^3 ng/mL, 1×10^3 ng/mL, 5×10^3 ng/mL, and the THz spectra of the control group and the control group at each adsorption time (6 h, 12 h, 18 h) were obtained. Fig. 2(a) corresponds to the spectra of Scenedesmus obliquus at different time points under seven different Pb^{2+} concentrations. Fig. 2(b) shows the spectra of microalgae under the stress of 5×10^3 ng/mL Pb^{2+} concentrations at 0 h, 6 h, 12 h and 18 h. All spectra form a large envelope at about 4.27 THz, corresponding to the two raised peaks at 9.24 THz and 10.57 THz, and there are obvious characteristic peaks at 17.5 THz. According to Section 3.1, the characteristic peak at 4.27 THz also corresponds to protein. Therefore, these four characteristic peaks correspond to proteins, lipids, polysaccharides and β-carotene in microalgae.
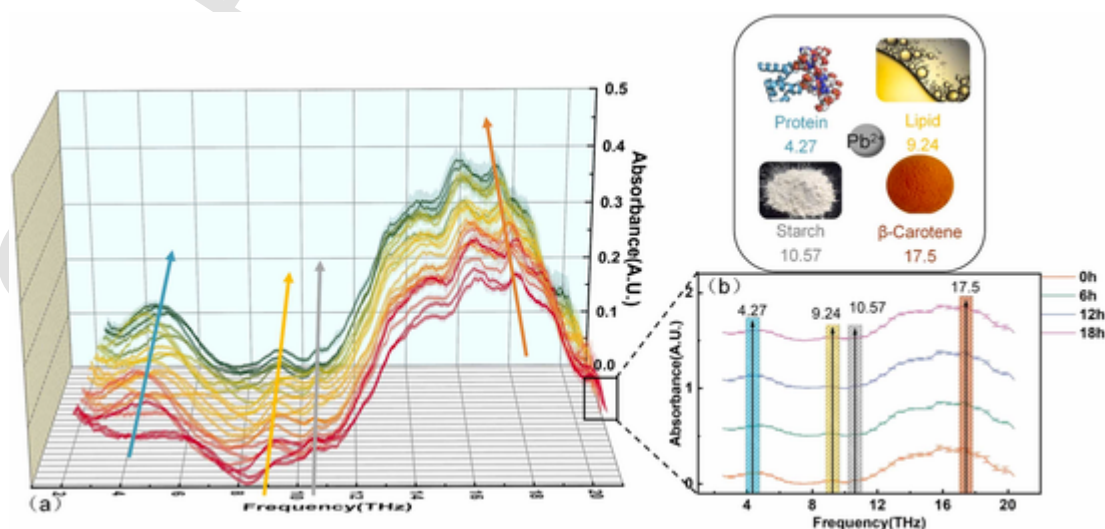
Fig. 2. (a) shows the spectra of microalgae under the stress of seven different Pb^{2+} concentrations at 0 h, 6 h, 12 h and 18 h. (b) shows the spectra of microalgae under the stress of 5×10^3 ng/mL Pb^{2+} concentrations at 0 h, 6 h, 12 h and 18 h.

3.3. Changes of main components in microalgae under Pb^{2+} Stress

3.3.1. Study on changes of substance composition in microalgae based on terahertz spectroscopy

We choose 0.5×10^3 ng/mL as the higher Pb^{2+} concentration, 50 ng/mL as the medium Pb^{2+} concentration, and 1 ng/mL as the lower Pb^{2+} concentration. We extracted four characteristic peaks of 4.27 THz, 9.24 THz, 10.57 THz and 17.5 THz, and studied the variation law of absorbance of these peaks with time (6 h, 12 h and 18 h), as shown in Fig. 3. According to the above spectral characteristics, in higher concentration Pb^{2+} solution, lipid, protein, starch and β-carotene all reach the lowest peak within 6 h, then they increase at 6–12 h and decrease at 12–18 h. According to the amplitude of absorbance, β-carotene changes the most, as shown in Fig. 3(a), (b) and (c). In the medium concentration Pb^{2+} solution, lipid, protein, starch and β-carotene decrease to 6 h, then they increase at 6–12 h and decrease at 12–18 h. We can see that the change amplitude of β-carotene is the largest, as shown in Fig. 3(d), (e) and (f). In the lower Pb^{2+} concentration, lipids, proteins, starch and

β-carotene show a slow decreasing trend until 12 h and then increase, as shown in Fig. 3(g), (h), and (i). We can see from the absorbance amplitude that β-carotene change the most.

3.3.2. Study on the composition change of microalgae based on PCA

In order to study the influence of Pb^{2+} on the main components of microalgae under different adsorption time. In the experiment, PCA was used to analyze the absorbance values corresponding to the spectral characteristic peaks of the main components of microalgae under Pb^{2+} stress. The absorption peak of starch is at 10.57 THz, the absorption peak of β-carotene is at 17.5 THz, the absorption peak of lipids is at 9.24 THz, and the absorption peak of protein is at 4.27 THz. We selected high, middle and low concentrations for analysis. In Fig. 4, the cumulative contribution rates of component 1 and component 2 are 100%, which is able to effectively distinguish microalgae samples at different adsorption time points. Fig. 4(a) shows the Bi-plot diagram of higher concentration. The clustering results of samples at 18 h indicate that it is closer to 9.24 THz, which is mainly affected by lipids at 18 h.
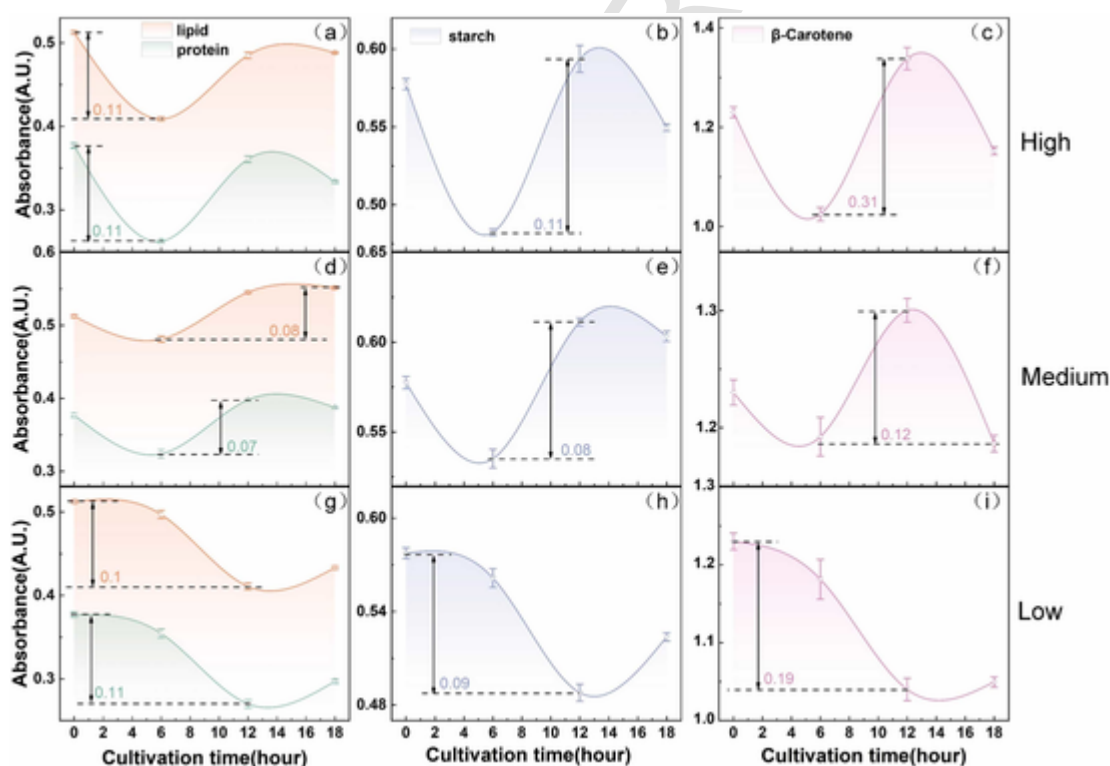
Fig. 3. (a), (b) and (c) show the spectra of microalgae lipids, protein, starch and β-carotene under high concentration (0.5×10^3 ng/mL) Pb^{2+} stress; (d),(e) and (f) show the spectra of microalgae lipid, protein, starch and β-carotene under medium concentration (50 ng/mL) Pb^{2+} stress; (g), (h) and (i) show the spectra of microalgae lipid, protein, starch and β-carotene under low concentration (1 ng/mL) Pb^{2+} stress.
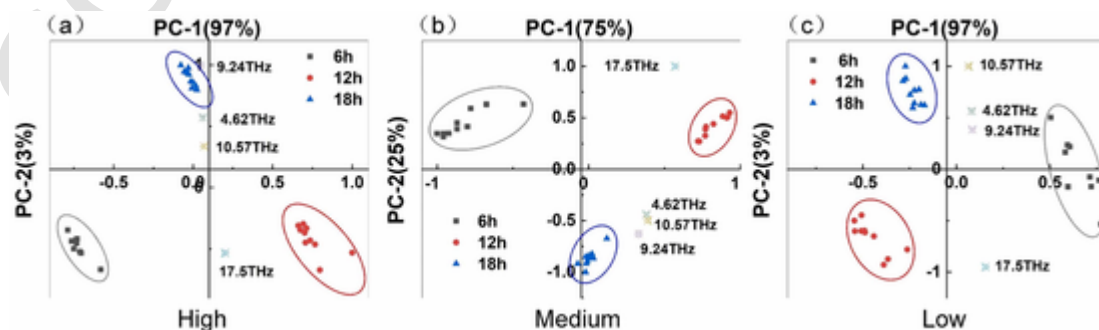
Fig. 4. (a) shows the PCA analysis result of high concentration (0.5×10^3 ng/mL) Pb^{2+} microalgae spectra; (b) shows the PCA analysis result of medium concentration (50 ng/mL) Pb^{2+} microalgae spectra; (c) shows the PCA analysis result of low concentration (1 ng/mL) Pb^{2+} microalgae spectra.

Compared with proteins at 4.27 THz and starch at 10.57 THz, β-carotene at 17.5 THz is more inclined to affect samples at 12 h. Fig. 4(b) shows the Bi-plot diagram for the medium concentration, in which the protein, lipid and starch represented at 4.27 THz, 9.24 THz and 10.57 THz tend to dominate the changes of 18 h samples, and the β-carotene represented at 17.5 THz affects the changes of 12 h samples, and the influence degree of protein, lipid and starch is the same as that of β-carotene in distance. Fig. 4(c) shows the Bi-plot diagram for the lower concentration, in which the protein, lipid and starch represented at 4.27 THz, 9.24 THz and 10.57 THz respectively tend to dominate the samples for 18 h, and the β-carotene represented at 17.5 THz tend to dominate the samples for 12 h. In terms of distance, the effects of protein, lipid, starch and β-carotene are the same. Based on the amplitude of spectral changes and the results of PCA cluster analysis, we still give priority to the leading role of β-carotene.

3.3.3. Trend analysis of β-carotene content in microalgae

Through the above principal component analysis, it is concluded that the changes caused by β-carotene content in the body are relatively significant in the process of Pb^{2+} stress. The variation trend of β-carotene content and terahertz spectrum is also compared and analyzed. We used the thermal ethanol method to extract β-carotene from experimental microalgae, and measured the content of β-carotene by spectrophotometer, as the true content value of β-carotene. Results As shown in Fig. 5(a), (b) and (c), in high concentration Pb^{2+} solution, the content of extracted β-carotene decreased from 2.45 mg/L to 2.15 mg/L within 6 h, then increased to 2.6 mg/L within 12 h, and then decreased. This is the same as the spectral trend in Section 3.3.1. In Pb^{2+} solution with medium concentration, the content of β-carotene decreased from 2.45 mg/L to 2.3 mg/L within 6 h, then increased to 2.45 mg/L within 12 h, and then decreased to 2.2 mg/L within 18 h. In Section 3.3.1, under the stress of medium lead ion concentration, β-carotene decreased in 6 h, increased in 6–12 h and decreased in 12–18 h. This concentration change trend is the same as that of β-carotene in this section. In the low concentration of Pb^{2+} solution, the β-carotene content decreased from 2.45 mg/L to 1.5 mg/L, with a gradual gentle trend. Compared with the spectral trend of low concentration lead ion stress in Section 3.3.1, both showed a downward trend within 12 h, the spectral data from 12 h to 18 h showed an increasing trend, and the traditional detection data showed a flat trend.

3.4. Establish a prediction model of Pb^{2+} concentration based on PLS at different time points

According to the above study, the β-carotene content in the microalgae under Pb^{2+} stress changes most obviously. Further, the absorbance values of microalgae samples at different time points in the range of 75–680 cm^{-1} were used to establish a prediction model of Pb^{2+} concentration based on PLS. When establishing the PLS prediction model, the PLS model matrix was also constructed according to the ratio of 2:1 be-

tween the correction set and the prediction set, and the corresponding assignments ("1", "2", "3", "4", "5", "6", "7") were set for the seven concentrations (1 ng/mL, 10 ng/mL, 50 ng/mL, 0.1×10^3 ng/mL, 0.5×10^3 ng/mL, 1×10^3 ng/mL, 5×10^3 ng/mL). The accuracy of the prediction model was determined by comparing the coefficient of determination and the root mean square error of the correction set and the prediction set.

The results of the model established by PLS are shown in Table 2. We can conclude that the modeling effect of PLS at 6 h is the best, and the results of 12 h and 18 h are also good, but the accuracy is less than that of 6 h.

3.5. Spectra of microalgae under Ni^{2+} solution stress

After determining the characteristic absorption peaks of the main substances in the microalgae, we performed terahertz spectra collection and peaks analysis on the samples of Scenedesmus obliquus after adsorbing Ni^{2+} in different concentrations of Ni^{2+} solutions in this study. The concentrations of Ni^{2+} in the solution are 1 ng/mL, 10 ng/mL, 50 ng/mL, 0.1×10^3 ng/mL, 0.5×10^3 ng/mL, 1×10^3 ng/mL and 3×10^3 ng/mL. the THz spectra of each time (6 h, 12 h and 18 h) and the control group (0 h) are detected by FTIR. Fig. 6 corresponds to the spectra of Scenedesmus obliquus at different time points under seven different Ni^{2+} concentrations. All spectra have a large envelope around 3.67 THz, and there are obvious characteristic peaks at 9.24 THz, 10.57 THz and 17.5 THz in the Fig. 6(a). Fig. 6(b) shows the spectra of microalgae under the stress of 3×10^3 ng/mL Ni^{2+} concentrations at 0 h, 6 h, 12 h and 18 h. According to Section 3.1, these four characteristic peaks correspond to proteins, lipids, polysaccharides and β-carotene in microalgae.

3.6. Changes of main components in microalgae under Ni^{2+} stress

3.6.1. Study on changes of substance composition in microalgae based on terahertz spectroscopy

In order to facilitate the analysis of the main substances in the microalgae, we choose 1×10^3 ng/mL as the higher Ni^{2+} concentration, 0.1×10^3 ng/mL as the medium Ni^{2+} concentration, and 10 ng/mL as the lower Ni^{2+} concentration. We extracted the characteristic peak information of 3.67 THz, 9.24 THz, 10.57 THz and 17.5 THz, and studied the change law of absorbance of these peaks with time (6 h, 12 h and 18 h), as shown in Fig. 7. According to the spectral characteristic, in relatively high concentrations (1×10^3 ng/mL) of Ni^{2+} in the solution, the lipid, protein, starch and β-carotene first increased to 6 h and then began to decrease. It can be seen that the spectral change of carotene is the largest among the four substances, as shown in Fig. 7(a), (b) and (c). In the solution with medium concentration of Ni^{2+}, the lipid, protein and starch decreased in 6 h and increased in 6–18 h. β-carotene began to increased in 6 h, decreased at 6–12 h, and increased again at 12–18 h, we can see from the absorbance amplitude that the β-carotene
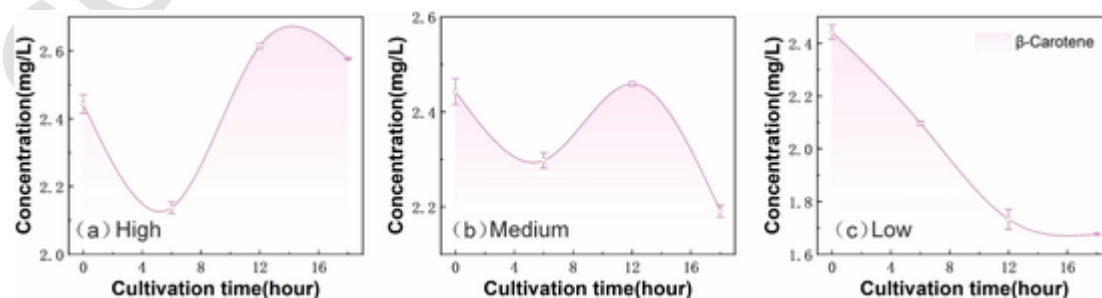
Fig. 5. (a) It is the change trend of chemical detection of β-carotene under medium concentration (0.5×10^3 ng/mL) Pb^{2+} stress; (b) It is the change trend of β-carotene in terahertz spectrum under medium concentration (50 ng/mL) Pb^{2+} stress; (c) It is the change trend of chemical detection of β-carotene under low concentration (1 ng/mL) Pb^{2+} stress.

Table 2
Prediction of Pb^{2+} concentration levels at different time based on PLS models.

Discrimination model	Calibration		Prediction	
	R_c^2	RMSEC	R_p^2	RMSEP
6 h	0.993	0.148	0.986	0.222
12 h	0.964	0.378	0.902	0.625
18 h	0.978	0.296	0.956	0.416

changes the most, as shown in Fig. 7(d), (e) and (f). In the solution with lower concentration of Ni^{2+}, the lipid, protein, starch and β-carotene show a decreasing trend, and then increase to 12 h and then decreased. This concentration of β-carotene decreases to 6 h and then slowly increases, as shown in Fig. 7(g), (h) and (i). We can see from the absorbance amplitude that the β-carotene changes the most. Compared with the influence of Pb^{2+}, Pb^{2+} has a greater impact on the spectra of β-carotene, while the spectra of proteins, lipids and starches are less affected.
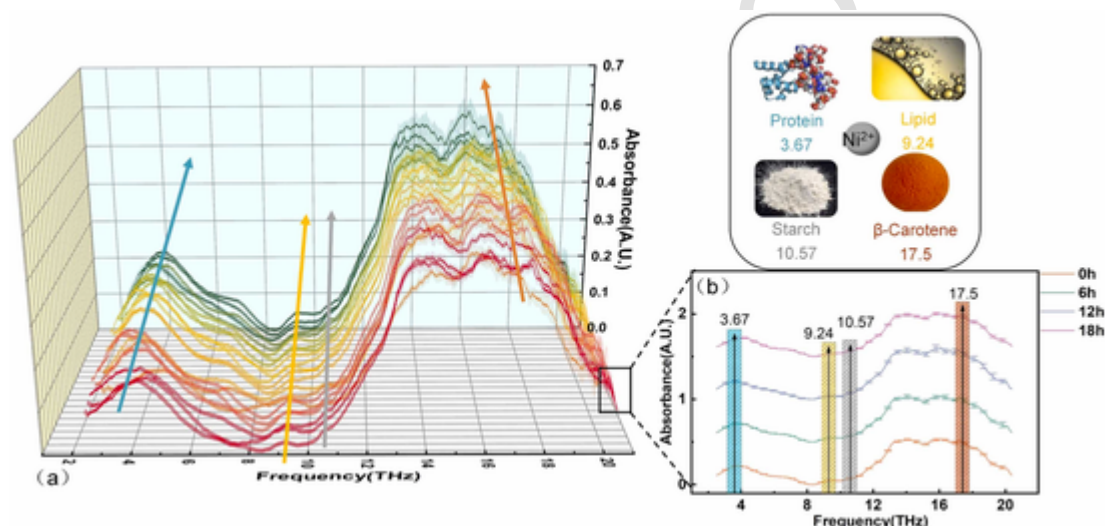
Fig. 6. (a) shows the spectra of microalgae under the stress of seven different Ni^{2+} concentrations at 0 h, 6 h, 12 h and 18 h; (b) shows the spectra of microalgae under the stress of 3×10^3 ng/mL Ni^{2+} concentrations at 0 h, 6 h, 12 h and 18 h.
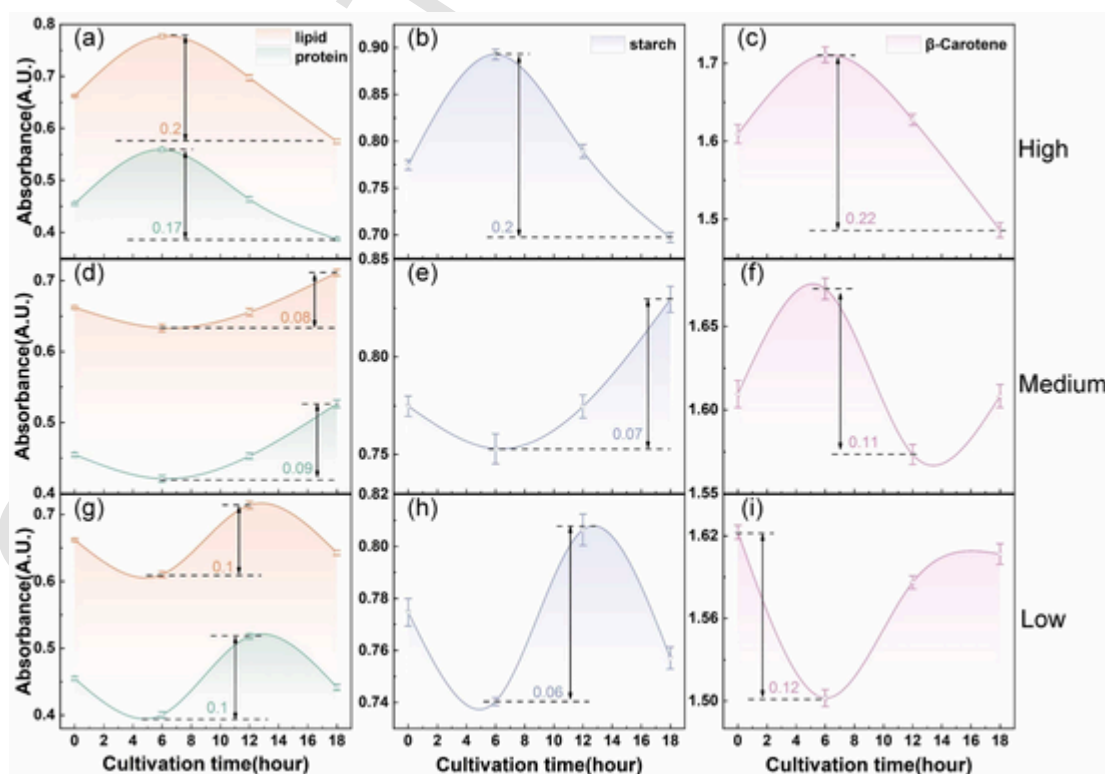
Fig. 7. (a),(b) and (c) show the spectra of lipid, protein, starch and β-carotene of Scenedesmus obliquus under high concentration (1×10^3 ng/mL) Ni^{2+} stress; (d), (e) and (f) show the spectra of lipid, protein, starch and β-carotene of Scenedesmus obliquus under medium concentration (0.1×10^3 ng/mL) Ni^{2+} stress; (g), (h) and (I) show the spectra of lipid, protein, starch and β-carotene of Scenedesmus obliquus under low concentration (10 ng/mL) Ni^{2+} stress.

3.6.2. Study on the composition change of microalgae based on PCA

In order to study the influence of Ni^{2+} on the main components in microalgae at different times, the absorbance values corresponding to the spectral characteristic peaks of the main constituents were analyzed via principal component analysis. The absorption peak of starch is at 10.57 THz, the absorption peak of β-carotene is at 17.5 THz, the absorption peak of lipids is at 9.24 THz, and the absorption peak of protein is at 3.67 THz. We selected high, medium and low concentrations for analysis. In Fig. 8, the cumulative contribution rates of component 1 and component 2 are 100%, which can effectively distinguish microalgae samples at different time points. Fig. 8(a) shows the Bi-plot diagram of higher concentration, in which the PCA results of 12 h samples are mainly affected by the absorbance value at 17.5 THz. Therefore, it is considered that microalgae have a great impact on the change of β-carotene content in vivo under high concentration Ni^{2+} stress. Fig. 8(b) shows the Bi-plot diagram for medium concentration, in which the PCA results of 6 h samples are mainly affected by the absorbance values at 3.67 THz, 9.24 THz and 17.5 THz. Therefore, it is considered that microalgae have a great impact on the changes of protein, lipids and β-carotene contents in vivo under medium concentration Ni^{2+} stress. Fig. 8(c) shows the Bi-plot diagram of low concentration, in which the PCA results of 18 h samples are mainly affected by the absorbance value at 17.5 THz. Therefore, it is considered that microalgae have a great impact on the change of β-carotene content in vivo under low concentration Ni^{2+} stress.

3.6.3. Trend analysis of β-carotene content in microalgae

Based on the above principal component analysis results, we concluded that the β-carotene content in Scenedesmus obliquus is significantly changed under Ni^{2+} stress. Therefore, the change trend of carotene content and terahertz spectrum was compared and analyzed. We extracted β-carotene from experimental microalgae by hot ethanol method, and measured their content by spectrophotometer as the real content of β-carotene. As shown in Fig. 9(a), (b) and (c), in high concentration Ni^{2+} solution, the content of extracted β-carotene increased

from 1.35 mg/L to 1.6 mg/L, and then gradually decreased to 1.2 mg/L, which was consistent with the spectral change trend in Section 3.6.1. In the medium concentration Ni^{2+} solution, the content of β-carotene increased from 1.35 mg/L to 1.85 mg/L within 6 h, then decreased to 1.55 mg/L and then increased to 1.64 mg/L within 12 h. This is consistent with the spectral changes in Section 3.6.1. In low concentration Ni^{2+} solution, the content of β-carotene decreased to 1.08 mg/L within 6 h, and then gradually increased to 1.7 mg/L. This trend is also the same as the spectral change in Section 3.6.1.

3.7. Establish a prediction model of Ni^{2+} concentration based on PLS at different time points

According to with the above study, the β-carotene content of microalgae under Ni^{2+} stress changes most remarkably. Further, we established a prediction model of Ni^{2+} concentration based on PLS based on the absorbance values of the samples of Scenedesmus obliquus in the range of 75–680 cm^{-1} at different adsorption time points within 18 h. We built PLS model according to the ratio of 2:1 between correction set and prediction set, and set corresponding assignments ("1", "2", "3", "4", "5", "6", "7") for seven concentrations (1 ng/mL, 10 ng/mL, 50 ng/mL, 0.1×10^3 ng/mL, 0.5×10^3 ng/mL, 1×10^3 ng/mL and 3×10^3 ng/mL). The accuracy of the prediction model is judged by comparing the coefficient of determination and the root mean square error of the correction set and the prediction set.

Based on the results of the model established by PLS as shown in Table 3, we can conclude that the accuracy of PLS modeling is getting better and better with the passage of time, and the best modeling value is reached by 18 h in the time we designed the experiment. Compared with Pb^{2+} model, Pb^{2+} model has significant effect in 6 h and better resolution effect in a short time, while Ni^{2+} model has better effect in 18 h, which is also consistent with the situation that Pb^{2+} toxicity is greater than Ni^{2+}.
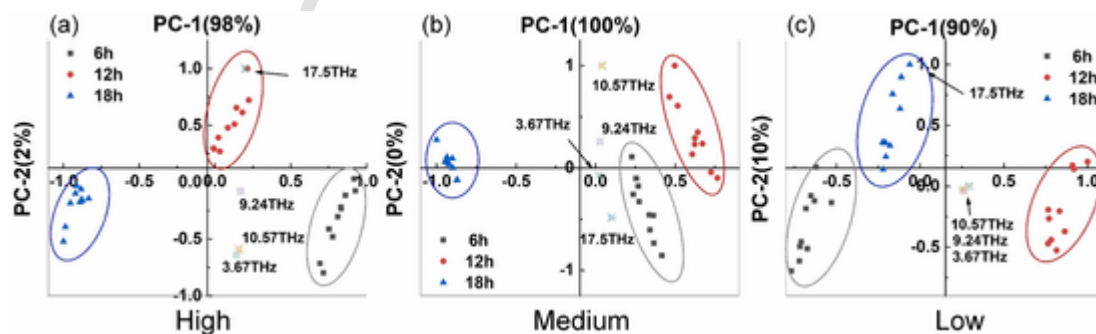
Fig. 8. (a) shows the PCA analysis result of high concentration (1×10^3 ng/mL) Ni^{2+} microalgae spectra; (b) shows the PCA analysis result of medium concentration (0.1×10^3 ng/mL) Ni^{2+} microalgae spectra; (c) shows the PCA analysis result of low concentration (10 ng/mL) Ni^{2+} microalgae spectra.
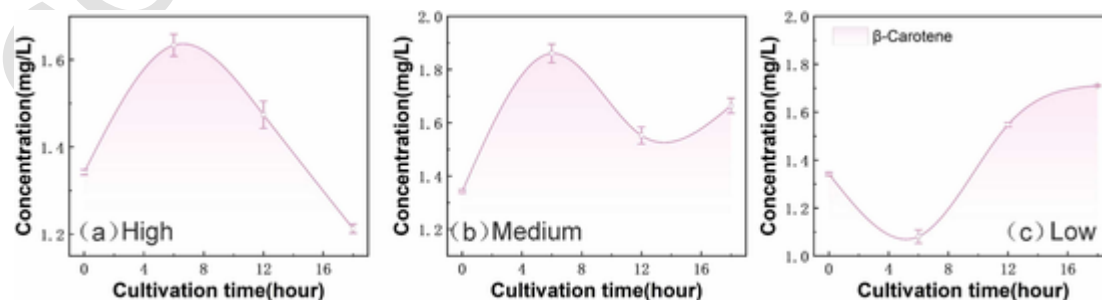
Fig. 9. (a) It is the change trend of chemical detection of β-carotene under medium concentration (1×10^3 ng/mL) Ni^{2+} stress; (b) It is the change trend of β-carotene in terahertz spectrum under medium concentration (0.1×10^3 ng/mL) Ni^{2+} stress; (c) It is the change trend of chemical detection of β-carotene under low concentration (10 ng/mL) Ni^{2+} stress.

Table 3

Prediction of Ni^{2+}concentration levels at different time based on PLS models.

Discrimination model	Calibration		Prediction	
	R_c^2	RMSEC	R_p^2	RMSEP
6 h	0.990	0.196	0.850	0.748
12 h	0.993	0.155	0.943	0.457
18 h	0.997	0.103	0.962	0.375

3.8. Establish a PLS-based prediction model for Pb^{2+} and Ni^{2+} mixed solutions with different concentrations

Based on the above spectral changes and cluster analysis, it was found that the spectrum of β-carotene was the most affected and dominant factor when Scenedesmus obliquus was stressed by Pb^{2+} and Ni^{2+}. According to the results of PLS modeling, the modeling effect of Pb^{2+} stress experiment at 6 h is the best, and that of Ni^{2+} stress experiment at 18 h is the best. Therefore, we designed a mixed solution of Pb^{2+} and Ni^{2+} with different concentrations to stress Scenedesmus obliquus, and selected two optimal time points of 6 h and 18 h. According to the concentration of Pb^{2+} and Ni^{2+} designed above, we selected the concentration of mixed heavy metal solution in the concentration range of the above single ion modeling, as shown in Table 4 (the selection of concentration in the table referred to the concentration of heavy metal ions in surface water in Section 3.9).

It has been known from the above experiments that β-carotene are the most affected and dominant factor in the spectrum. Therefore, in the mixed solution stress experiment, a band model containing only β-carotene was adopted (15–18 THz was selected). During modeling, the samples were marked as "1", "2", "3" and "4", and the accuracy of the prediction model was determined by comparing the coefficient of determination and root mean square error of the correction set and the prediction set.

According to Table 5, the coefficient of determination of calibration (R_c^2) at 6 h is 0.989 and the root mean square error of calibration (RMSEC) is 0.116, the coefficient of determination of prediction (R_p^2) is 0.991 and the root mean square error of prediction (RMSEP) is 0.102. The coefficient of determination of calibration (R_c^2) at 18 h is 0.883 and the root mean square error of calibration (RMSEC) is 0.381, the coefficient of determination of prediction (R_p^2) is 0.979 and the root mean square error of prediction (RMSEP) is 0.161. According to the coefficient of determination of calibration and the coefficient of determination of prediction in the model results of PLS of Pb^{2+} experiment in Table 2, the best time is 6 h, and according to the coefficient of determination of calibration and the coefficient of determination of prediction in the model results of PLS of Ni^{2+} experiment in Table 3, the best time

is 18 h. Therefore, we believe that 6 h is the judgment time of Pb^{2+} and 18 h is the judgment time of Ni^{2+}.

3.9. Study on concentration of Ni^{2+} and Pb^{2+} in real surface water based on PLS

In order to verify the prediction accuracy and reliability of the mixed solution model in Section 3.8, we selected several representative surface water samples, which were taken from Yangcheng Lake water sample, Suzhou battery plant wastewater sample (after wastewater treatment), Taihu Lake water sample, Chaohu Lake water sample and Hongze Lake water sample. We adopted the atomic absorption spectrometry to detect the Ni^{2+} and Pb^{2+} content of these five water samples, The result shows that the Pb^{2+} content of the five kinds of real surface water is 10 ng/mL and the Ni^{2+} content is 50 ng/mL. Then we placed *Scenedesmus obliquus* into these five surface waters for adsorption culture, 6 samples per surface water, a total of 30 samples, sampling at 6 h and 18 h and collecting terahertz spectra at 15–18 THz bands. The collected 30 spectral data were predicted by PLS model, and the prediction threshold was set to 0.5. The samples predicted as "1" were the samples stressed by the mixed solution of 50 ng/mL Ni^{2+} and 10 ng/mL Pb^{2+}.

It can be seen from Table 6 that when the PLS prediction threshold is 0.5, the Pb^{2+}(6 h) judgment accuracy of samples from Taihu Lake, Hongze Lake, Suzhou battery plant treated sewage, Yangcheng Lake and Chaohu Lake reaches 100%, and the Ni^{2+}(18 h) judgment accuracy of samples from Suzhou battery plant treated sewage, Yangcheng Lake and Chaohu Lake reaches 100%. The accuracy of Ni^{2+}(18 h) in Taihu Lake and Hongze Lake samples was 83%. Therefore, it is concluded that in this experiment, the prediction accuracy of Pb^{2+} is 100%, and that of Ni^{2+} is 93.2%. This result also confirmed that the Pb^{2+} with greater toxicity had a higher impact on microalgae, which was easier to be detected in a short time than Ni^{2+}. We compared some parameters of other traditional methods and this experiment, as shown in Table 1.

4. Conclusion

In this study, the terahertz spectra were collected under the stress of two different toxic heavy metals (Pb^{2+} and Ni^{2+}) at different time (0 h, 6 h, 12 h, 18 h), and the changes of protein, lipid, starch and β-carotene content in microalgae were analyzed by using the spectral information. At the same time, combined with PCA, chemical methods and PLS analysis, it is concluded that the time for judging lead ions is 6 h, the time for judging nickel ions is 18 h, and the characteristic substance is β-carotene (15–18 THz). Then, the PLS model was established through the mixed heavy metal ions stress microalgae experiment with the above time and band, combined with surface water to verify the model, the accuracy of the judgment for Pb^{2+} was 100%, and the judgment accuracy for Ni^{2+} was 93.2%. This also verifies that the toxicity of Pb^{2+} is greater than that of Ni^{2+}. After establishing the PLS model in this method, the detection of water bodies does not require the use of chemical means to carry out complicated pretreatment of the samples, and only about 10 mL of water samples are needed to detect the stress microalgae by terahertz spectroscopy. We provide a new detection ap-

Table 4

Mixing ratio of Pb^{2+} and Ni^{2+}.

Samples	Ni^{2+}	Pb^{2+}
1	50 ng/mL	10 ng/mL
2	0.5×10^3 ng/mL	10 ng/mL
3	50 ng/mL	0.1×10^3 ng/mL
4	0.5×10^3 ng/mL	0.1×10^3 ng/mL

Table 5

Prediction of mixed concentration at different time based on PLS models.

Discrimination model	Calibration		Prediction	
	R_c^2	RMSEC	R_p^2	RMSEP
6 h	0.989	0.116	0.991	0.102
18 h	0.883	0.381	0.979	0.161

Table 6

Surface water determination accuracy based on PLS model (threshold "0.5").

Accuracy	Pb^{2+} (6 h)	Ni^{2+} (18 h)
Taihu Lake	100%	83%
Hongze Lake	100%	83%
Suzhou	100%	100%
Yangcheng Lake	100%	100%
Chaohu Lake	100%	100%
Summary	100%	93.2%

proach and technical support for the real-time monitoring of the types and concentrations of heavy metals in water.

CRediT authorship contribution statement

Declaration of Competing Interest

The authors declare that they have no known competing financial interests or personal relationships that could have appeared to influence the work reported in this paper.

Acknowledgements

Environmental implication

Heavy metals lead and nickel have been internationally recognized as harmful metals to human body, especially in urban wastewater and industrial wastewater. Therefore, a more convenient and fast detection method is needed. We choose to use microalgae in the environment to adsorb heavy metals, and infer the concentration and species of heavy metals in water by terahertz spectroscopy. It provides a new idea for the detection of heavy metals in water.

References

Adhiya, J., Cai, X.H., Sayre, R.T., Traina, S.J., 2002. Binding of aqueous cadmium by the lyophilized biomass of Chlamydomonas reinhardtii. Colloids Surf. -Physicochem. Eng. Aspects 210 (1), 1–11.

Dean, A.P., Sigee, D.C., Estrada, B., Pittman, J.K., 2010. Using FTIR spectroscopy for rapid determination of lipid accumulation in response to nitrogen limitation in freshwater microalgae. Bioresour. Technol. 101 (12), 4499–4507.

Doshi, H., Ray, A., Kothari, I.L., Gami, B., 2006. Spectroscopic and scanning electron microscopy studies of bioaccumulation of pollutants by algae. Curr. Microbiol. 53 (2), 148–157.

Filote, C., Volf, I., Santos, S.C.R., Botelho, C.M.S., 2019. Bioadsorptive removal of Pb(II) from aqueous solution by the biorefinery waste of Fucus spiralis. Sci. Total Environ. 648, 1201–1209.

Flores-Morales, A., Jimenez-Estrada, M., Mora-Escobedo, R., 2012. Determination of the structural changes by FT-IR, Raman, and CP/MAS (13)C NMR spectroscopy on retrograded starch of maize tortillas. Carbohydr. Polym. 87 (1), 61–68.

Indhumathi, P., Sathiyaraj, S., Koelmel, J.P., Shoba, S.U., Jayabalakrishnan, C., Saravanabhavan, M., 2018. The efficient removal of heavy metal ions from industry effluents using waste biomass as low-cost adsorbent: thermodynamic and kinetic models. Zeitschrift für Physikalische Chem. 232 (4), 527–543.

Ji, Y., He, Y., Cui, Y., Wang, T., Wang, Y., Li, Y., Huang, W.E., Xu, J., 2014. Raman spectroscopy provides a rapid, non-invasive method for quantitation of starch in live, unicellular microalgae. Biotechnol. J. 9 (12), 1512–1518.

Jiang, F.L., Ikeda, I., Ogawa, Y., Endo, Y., 2011. Terahertz absorption spectra of Fatty acids and their analogues. J. OLEO Sci. 60 (7), 339.

Kim, J.J., Kim, Y.S., Kumar, V., 2019. Heavy metal toxicity: An update of chelating therapeutic strategies. J Trace Elem Med Biol 54, 226–231.

Kobielska, P.A., Howarth, A.J., Farha, O.K., Nayak, S., 2018. Metal–organic frameworks for heavy metal removal from water. Coord. Chem. Rev. 358, 92–107.

Leborans, G.F., Novillo, A., 1996. Toxicity and bioaccumulation of cadmium in Olisthodiscus luteus (Raphidophyceae). Water Res. 30 (1), 57–62.

Ling, F., Jiang, Ikuo, Ikeda, Yuichi, Ogawa, Yasushi, Endo, 2012. Rapid determination of saponification value and polymer content of vegetable and fish oils by terahertz spectroscopy. J. OLEO Sci.

Ljungqvist, M.G., Nielsen, O.H.A., Frosch, S., Nielsen, M.E., Clemmensen, L.H., Ersbøll, B.K., 2013. Hyperspectral imaging based on diffused laser light for prediction of astaxanthin coating concentration. Mach. Vis. Appl. 25 (2), 327–343.

Lohumi, S., Lee, S., Lee, H., Cho, B.-K., 2015. A review of vibrational spectroscopic techniques for the detection of food authenticity and adulteration. Trends Food Sci. Technol. 46 (1), 85–98.

Magwaza, L.S., Opara, U.L., Nieuwoudt, H., Cronje, P.J.R., Saeys, W., Nicolai, B., 2012. NIR spectroscopy applications for internal and external quality analysis of citrus fruit- a review. Food Bioprocess Technol. 5 (2), 425–444.

Mangadze, T., Dalu, T., William Froneman, P., 2019. Biological monitoring in southern Africa: a review of the current status, challenges and future prospects. Sci. Total Environ. 648, 1492–1499.

Mathew, B.B. and Krishnamurthy, N.B. 2015. Health effects caused by metal contaminated ground water.

Nakajima, S., Shiraga, K., Suzuki, T., Kondo, N., Ogawa, Y., 2019. Quantification of starch content in germinating mung bean seedlings by terahertz spectroscopy. Food Chem. 294, 203–208.

Ogburn, Z.L., Vogt, F., 2017. Microalgae as embedded environmental monitors. Anal. Chim. Acta 954, 1–13.

Patel, A., Antonopoulou, I., Enman, J., Rova, U., Christakopoulos, P., Matsakas, L., 2019. Lipids detection and quantification in oleaginous microorganisms: an overview of the current state of the art. BMC Chem. Eng. 1 (1).

Peng, Y., Shi, C., Wu, X., Zhu, Y., Zhuang, S., 2020a. Terahertz imaging and spectroscopy in cancer diagnostics:a technical review. BME Front. 1 (1), 11.

Peng, Y., Shi, C., Zhu, Y., Gu, M., Zhuang, S., 2020b. Terahertz spectroscopy in biomedical field: a review on signal-to-noise ratio improvement. PhotoniX 1 (1).

Piotrowska-Niczyporuk, A., Bajguz, A., Talarek, M., Bralska, M., Zambrzycka, E., 2015. The effect of lead on the growth, content of primary metabolites, and antioxidant response of green alga Acutodesmus obliquus (Chlorophyceae). Environ. Sci. Pollut. Res. Int. 22 (23), 19112–19123.

Rekhi, H., Rani, S., Sharma, N., Malik, A.K., 2017. A review on recent applications of high- performance liquid chromatography in metal determination and speciation analysis. Crit. Rev. Anal. Chem. 47 (6), 524–537.

Shao, Y., Liu, J., Zhu, Z., Wang, Y., Zhu, Y., Peng, Y., 2021a. Quantitative detection on metabolites of Haematococcus pluvialis by terahertz spectroscopy. Comput. Electron. Agric. 186.

Shao, Y., Pan, J., Zhang, C., Jiang, L., He, Y., 2015. Detection in situ of carotenoid in microalgae by transmission spectroscopy. Comput. Electron. Agric. 112, 121–127.

Shao, Y., Wang, Y., Zhu, Z., Liu, J., Xiong, X., Zhu, Y., Zhai, R., Gu, M., Tian, Z., Peng, Y., 2021b. Quantification analysis of progesterone based on terahertz spectroscopy. IEEE Trans. Terahertz Sci. Technol. 11 (5), 519–526.

Stehle, C.U., Abuillan, W., Gompf, B., Dressel, M., 2012. Far-infrared spectroscopy on free- standing protein films under defined temperature and hydration control. J. Chem. Phys. 136 (7), 075102.

Subramaniyam, V., Subashchandrabose, S.R., Thavamani, P., Chen, Z., Krishnamurti, G.S.R., Naidu, R., Megharaj, M., 2016. Toxicity and bioaccumulation of iron in soil microalgae. J. Appl. Phycol. 28 (5), 2767–2776.

Sultana, N., Hossain, S.M.Z., Mohammed, M.E., Irfan, M.F., Haq, B., Faruque, M.O., Razzak, S.A., Hossain, M.M., 2020. Experimental study and parameters optimization of microalgae based heavy metals removal process using a hybrid response surface methodology-crow search algorithm. Sci. Rep. 10 (1), 15068.

Wallays, C., Missotten, B., De Baerdemaeker, J., Saeys, W., 2009. Hyperspectral waveband selection for on-line measurement of grain cleanness. Biosyst. Eng. 104 (1), 1–7.

Wang, C., Gong, J., Xing, Q., Li, Y., Liu, F., Zhao, X., Chai, L., Wang, C., Zheltikov, A.M., 2010. Application of terahertz time-domain spectroscopy in intracellular metabolite detection. J Biophotonics 3 (10–11), 641–645.

Xing, J., Symons, S., Shahin, M., Hatcher, D., 2010. Detection of sprout damage in Canada Western Red Spring wheat with multiple wavebands using visible/near-infrared hyperspectral imaging. Biosyst. Eng. 106 (2), 188–194.

Yang, X., Zhao, X., Yang, K., Liu, Y., Liu, Y., Fu, W., Luo, Y., 2016. Biomedical applications of terahertz spectroscopy and imaging. Trends Biotechnol. 34 (10), 810–824.

Zhang, C., Zuo, J., Zhang, X.-C., Zhang, L., Yu, F., Siegel, P.H., He, L., Zhang, Z., Zhang, C. and Shi, S.-C. 2010 The observation of terahertz spectra of all-trans beta-carotene molecule.